

Contact angle measurement with a smartphone

H. Chen,^{1,a)} Jesus L. Muros-Cobos,^{1,2,a)} and A. Amirfazli^{1,b)}

¹Department of Mechanical Engineering, York University, Toronto, Ontario M3J 1P3, Canada

²Department of Software Engineering, University of Granada, Granada 18010, Spain

(Received 14 January 2018; accepted 3 March 2018; published online 30 March 2018)

In this study, a smartphone-based contact angle measurement instrument was developed. Compared with the traditional measurement instruments, this instrument has the advantage of simplicity, compact size, and portability. An automatic contact point detection algorithm was developed to allow the instrument to correctly detect the drop contact points. Two different contact angle calculation methods, Young-Laplace and polynomial fitting methods, were implemented in this instrument. The performance of this instrument was tested first with ideal synthetic drop profiles. It was shown that the accuracy of the new system with ideal synthetic drop profiles can reach 0.01% with both Young-Laplace and polynomial fitting methods. Conducting experiments to measure both static and dynamic (advancing and receding) contact angles with the developed instrument, we found that the smartphone-based instrument can provide accurate and practical measurement results as the traditional commercial instruments. The successful demonstration of use of a smartphone (mobile phone) to conduct contact angle measurement is a significant advancement in the field as it breaks the dominate mold of use of a computer and a bench bound setup for such systems since their appearance in 1980s. *Published by AIP Publishing.* <https://doi.org/10.1063/1.5022370>

I. INTRODUCTION

When a drop of a liquid is placed on a solid surface, the angle at which the liquid-vapour (normally air) interface meets the solid surface is called the contact angle.^{1,2} This angle is an important physical parameter in surface science and is a manifestation of the molecular interaction between the liquid of the drop and the solid surface.²⁻⁶ Therefore, the value of the contact angle is important to study and understand different liquid solid interactions. For example, measuring the contact angle of a liquid (e.g., water) on a surface is widely utilized for surface quality control in coating industry and detection of surface contaminants (e.g., semiconductor industry).

Ideally, when a liquid drop is placed on a solid surface, a unique angle exists between the liquid and the solid surface. The value of this ideal contact angle (the so-called Young's contact angle) can be calculated using Young's equation.¹ However, in practice, due to the surface geometry, roughness, heterogeneity, contamination, and deformation, the value of the contact angle on a surface is not necessary a unique value but falls in a range. The upper and lower limits of this range are called the advancing contact angle (θ_a) and the receding contact angle (θ_r), respectively.^{7,8} Knowing θ_a and θ_r of a surface is of great scientific and practical importance since, for example, the adhesion force of a droplet onto a surface can be estimated knowing this value.⁹ Interested readers can find details about common and accurate terminology regarding contact angles in Ref. 10.

Given the importance of the contact angle in different applications, a number of methods were developed to measure

the contact angle: optical methods (e.g., drop shape analysis method), tilting plate method, Wilhelmy plate method, and so on.^{1,11,12} Among these methods, optical methods using a sessile droplet are the most widely used method. The sessile drop method has the advantages of ease of use, direct visualization, and a small volume and surface sample requirement. Guidelines to measurements of reproducible contact angles using a sessile-drop technique can be found in Ref. 13.

An instrument using optical methods for contact angle measurement typically has two subsystems. The first subsystem (named as hardware subsystem) is used to hold the solid surface, generate a drop, and capture the drop image on a solid surface. The second subsystem (named as software subsystem) is for image analysis and contact angle calculation. The typical arrangement of the hardware subsystem is shown in Fig. 1.

For conducting contact angle measurement, a liquid drop is first placed on the target surface. An image of drop is taken using a camera (with a lens system) that is backlit with a diffused light. The software subsystem analyzes this drop image and calculates the contact angle value.

Depending on the approaches for drop profile identification and angle calculation, the software subsystem can have two versions: manual or automatic version. For the manual version, an operator detects the drop profile visually (e.g., by selecting points on the drop outline; see Fig. 2) and then measures the contact angle manually using an image analysis program, e.g., Image J.¹⁴ Since the performance of the manual version is strongly dependent on the operator's experience, the measuring results are subjective. To remove subjectivity, many commercial instruments use an automatic version, i.e., the drop profile and the contact points are first identified automatically from the drop image through use of an image analysis algorithm. A certain function is then fitted to the drop profile and its tangent/slop is found at the contact points

^{a)}H. Chen and J. L. Muros-Cobos contributed equally to this work.

^{b)}Author to whom correspondence should be addressed: alidad2@yorku.ca.
Tel.: +1-416-736-5901.

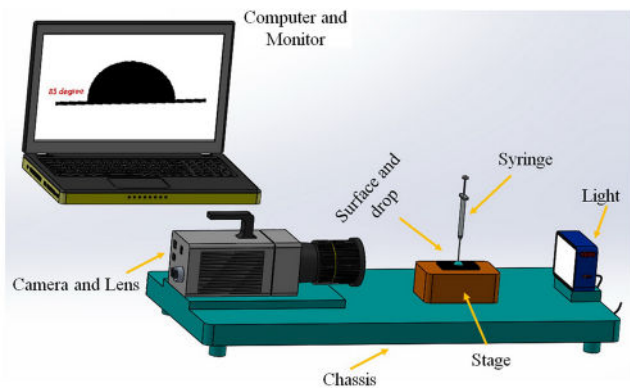


FIG. 1. Schematic of a setup for measuring contact angle using the optical method.

to calculate the contact angle (see Fig. 2). One of the most widely used fitting methods is called the Young-Laplace fitting method [Fig. 2(a)]. For a drop sitting on a surface, the profile of the drop is described by the Young-Laplace equation.¹⁵ Therefore, a possible ideal shape obtained from the Young-Laplace equation [the red solid line in Fig. 2(a)], which best fits the detected drop profile [red cross points in Fig. 2(a)], can be obtained. The contact angle can then be calculated as the angle between the surface and the tangent to this profile at the contact points. The Young-Laplace fitting method can only work with an axisymmetric drop; however, an axisymmetric drop is not always seen in practice. For example, for θ_a and θ_r measurement, a needle is typically inserted into the drop to increase or decrease the drop volume [see Fig. 2(b)]. Due to the presence of a needle, the drop profile may not be axisymmetric. Therefore, other fitting methods were developed for these drops. Among them is the polynomial fitting (fit the detected drop profile with a second order polynomial) which has the advantages of high-accuracy and low computational cost.¹⁶ For polynomial fitting, instead of using the whole drop profile, only part of the drop profile [the green points in Fig. 2(b)] is used, e.g., with a second order polynomial (green solid line in Fig. 2).

Thus, based on the discussion above, current contact angle measurement instruments (with optical method) consist of a liquid drop generation system, an optical system (typically a CCD camera coupled to a zoom lenses system) and chassis to hold them all together, as well as, a computational unit, data display, and storage system (e.g., a computer).

With such an arrangement, a traditional/current measurement instrument is heavy, bulky, and expensive; such arrangement makes the contact angle measurement system bench bound and not suitable for *in situ* or field work. Another main usage of the contact angle measurement instrument is for education. As an important physical parameter, the concept of the contact angle as well as related concepts needs to be taught to students in physics, chemistry, and engineer programs. However, due to the high cost of the traditional instruments, such measurement instrument is not typically accessible to most of the students. Therefore, it is clear that a compact and relatively low cost contact angle measurement instrument is needed for both field measurement and educational purposes.

With the fast development of the smartphone technology, a typical smartphone has a powerful central processing unit (CPU), a display screen, storage, and an image acquisition system (camera and lens). Essentially, both the bulky and expensive optical and process systems of the traditional contact angle measurement instrument are imbedded in a small and portable smartphone; hence, it gives the opportunity to build a small compact contact angle measurement instrument. A few attempts were made using smartphones to measure contact angles. However, in these attempts, e.g., Ref. 17, the smartphone was only used as a camera (extra lens and computer were needed for image capture and subsequent analysis, respectively). The accuracy of the measurement results were also not discussed satisfactorily.

The goal of this study is to develop a contact angle measurement instrument based on a smartphone platform (without extra lens and computer) which can have the similar performance as the best of the traditional instruments. This instrument should provide accurate measurement results for static contact angle of a drop on a solid surface and θ_a and θ_r between a liquid and a solid surface (need to take a series of drop images for the measurement).

One critical technical challenge for measuring contact angle using a smartphone (or even for any of the current automatic instruments) is to correctly identify the drop profile and especially the contact points. Compared with the traditional instruments which have an optical zoom system, a smartphone typically uses a digital zoom system. The drop edge in a digitally zoomed picture is usually not as well defined as an optically zoomed image. For example, in Ref. 18, we used a smartphone to measure the surface tension (calculating the

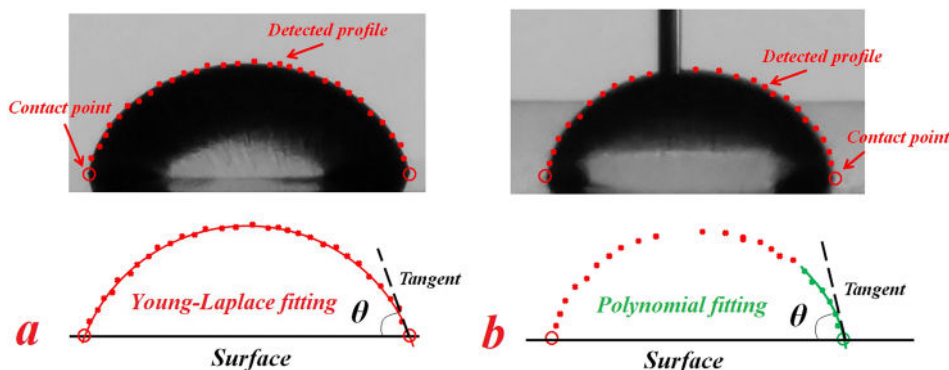


FIG. 2. Schematic for automatic optical method for contact angle measurement: (a) Young-Laplace fitting method and (b) polynomial fitting method.

surface tension value by using the profile of the droplet hanging from a capillary). It was shown that the traditional image analysis method, e.g., Canny method, cannot identify the drop profile correctly due to the fuzzy edge of the drop profile. Therefore, special attention needs to be paid to image analysis algorithm so it can work with a digitally zoomed image. Compared with the surface tension measurement, the contact angle measurement is more challenging for implementation in a smartphone. First, the performance of contact angle measurement is strongly dependent on the accuracy of the detection of contact points.^{1,14,16} However, the image of the drop close to surface is typically more challenging to be found when a digitally zoom picture is used. Second, the image involved in the contact angle measurement is more complicated compared with the ones used in the surface tension measurement. For example, for the advancing and receding measurements, a needle is usually inserted into drop to increase or decrease the drop volume. The presence of the needle adds to the difficulties for the drop profile detection. Therefore, different algorithms from our previous work in Ref. 18 are needed for different types of contact angle measurements.

The accuracy of an instrument is very important. Based on the definition, the accuracy of a measurement refers to the difference between a measured value and a standard or known value. As discussed before, when a drop is placed on a solid surface, the contact angle between the drop and the surface can be any value between θ_a and θ_r . In other words, the contact angle of a specific drop sitting on a surface is not a standard or deterministic value which can be used for calculating the accuracy. The value of θ_a and θ_r for a solid surface is also very sensitive and can be affected by many parameters, e.g., temperature, humidity, homogeneity, and minute contamination of the surface and liquid. For example, the advancing and receding contact angles of a surface at different locations can be different. Therefore, it is extremely difficult to find a standard or known value for calculating the accuracy of a contact angle measurement through a practical measurement. This is the reason that the parameter of accuracy is not provided by some of the commercial contact angle instruments in the market.

An alternate approach to find the accuracy of a contact angle measurement method or instrument is by using a synthetic drop.¹⁹ Synthetic drops are generated with a known value of contact angle. The accuracy of the measurement can be obtained by comparing the measured value and the value used to create the synthetic drop image.

In this study, a smartphone (mobile phone) based contact angle measurement instrument is presented. We selected the Android operating system as it is the most widespread operating system. Two different contact angle calculation algorithms (Young-Laplace and polynomial fitting methods) were applied to satisfy different measurement requirements. The accuracy of this instrument (with both fitting methods) was tested with synthetic drops (ideal drop profile). Finally, practical surface contact angle measurements were conducted using the smartphone-based instrument. The practical measurement results obtained from our instruments were compared with a high-end traditional commercial instrument to demonstrate utility.

II. METHODS

A. Software subsystem

The software of this instrument consists of two parts: image analysis and contact angle calculation parts. The majority of image analysis strategy is similar to our previous work,¹⁸ e.g., Otsu's algorithm is used to obtain the drop profile from digitally zoomed images. However, as discussed in the Introduction, the accuracy of the contact angle measurement is strongly dependent on the correct detection of the contact points. A usual strategy for detecting contact points is user intervention for one of the images in a series. The intervention usually takes the form of identifying the solid surface, e.g., drawing a horizontal line or on screen selecting of contact points by clicking on them on an image editor screen. If a line is used, the intersections between this line and the detected drop profile reveal the contact points. However, since the position to place the contact line is subjective, the performance of the measurement will rely on the users' experience, so there will be subjectively.

Based on the discussion above, an automatic contact point detection system which is not dependent on the operator's experience is needed. In practical measurements, depending on the solid surface and lighting conditions, the liquid drop can have a reflection [Fig. 3(a)] or not [Fig. 3(b)]. Therefore, the automatic contact point detection system should work for both types of images. For a drop image with reflection, the drop as well as its reflection profile can be detected [see Fig. 3(a)] by the image analysis algorithm. Considering the profile as a function, the slope of this function will change its sign (either from positive to negative or negative to positive) at the contact point. For a drop image without reflection, the slope of the drop profile will become zero after the contact point. Therefore, the contact points of a drop can be detected by checking the slope of the drop profile.

To check the slope of the drop profile close to the contact point, a point of the drop profile close to the contact point needs to be first identified. In our system, this point (first point) is found by asking the user to provide an estimated position of the contact line (point on the screen of the smartphone, shown as the red dashed line in Fig. 3). The intersection point between the drop profile and this estimated contact line is then identified automatically. As the estimated position for the contact line does not need to be too accurate, so subjectivity is not an issue. The line can be placed lower than the solid surface; hence, it is possible that no intersection point can be found. To ensure that the program can always detect a first point in the drop profile, the first point is found as 5% of the image height that is higher than the intersection point [see Fig. 3(a)]. A second and third drop profile points which are 10 pixels and 20 pixels lower than the first point, respectively, can be identified automatically. It should be noted that these numbers (e.g., 5% and 10 pixels) are selected based on empirical tests with a large number (~100) of experimental images. The slope between the first and second points (slope one, m_1), and second and third points (slope two, m_2) can be calculated and compared. Three possible scenarios can exist. First, if $m_1 \times m_2 < 0$, the contact point is in between the first and the third points (the first and third points are the point of drop profile and reflection, respectively). Second, if

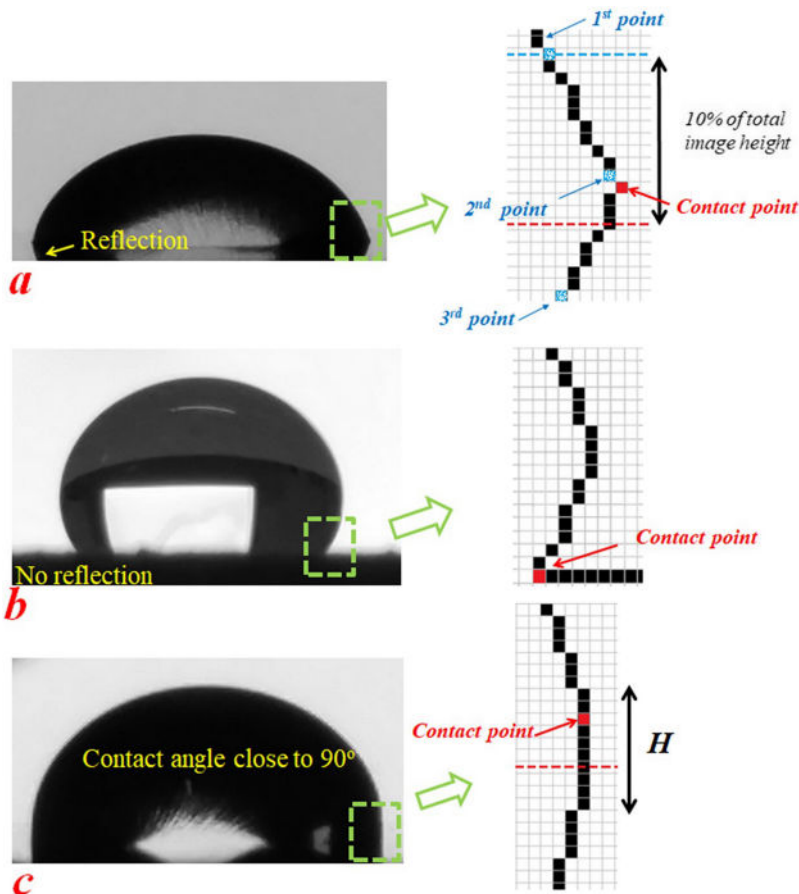


FIG. 3. Schematic for principle of contact point detection system: (a) an image of a drop with reflection, (b) an image of a drop without reflection, and (c) a drop with contact angle close to 90° . The right column shows digitally detected profiles (the dashed box shows estimated area to guide the eyes).

m_2 is close to 0° , the contact point is between the first and the second points (no reflection of drop). For both of these two scenarios, algorithms are applied to evaluate the slope of each neighbouring point in the range and find the points where the sign of slope starts to change (scenario one) or the slope becomes zero (scenario two) to seek the contact point.

It should be noted that for a drop with contact angle close to 90° , the drop profile close to the contact points can be perpendicular to the solid surface. Therefore, the sign of the drop profile may not change. To find the contact points for such drop images, the program will check the number of continuous neighbour profile points that have the same X (horizontal) coordinates as the intersection point. If there are more than eight continuous neighbouring profile points having the same X (horizontal) coordinates as the intersection point [i.e., $H \geq 8$ in Fig. 3(c)], the surface should have a contact angle of 90° or close to 90° . In such situations, the contact point is selected as the point located at one third of the profile points among these drop profiles (again based on tests with ~ 100 images).

Once the contact points are detected, the contact angle is the angle between the tangent of the drop profile and horizontal plane at the contact point. The tangent of the drop profile was obtained by fitting first the drop profile points detected and by the image analysis with either the Young-Laplace or a second order polynomial function. Then to calculate the contact angle, the slope of the fitted curve was found by differentiation using the coordinates of contact points.

The Young-Laplace fitting method finds a theoretical profile that best matches the drop profile exacted from the image and calculates the contact angle using this best matching profile. To calculate the drop profile using the Young-Laplace equation, the values of liquid density ($\Delta\rho$), gravity acceleration (g), liquid surface tension (γ), the total length of the drop profile (s), and the Laplace pressure difference (ΔP) are needed.¹⁵ The values of $\Delta\rho$ and g are needed as the initial inputs. Initial guessed values for γ , s , and ΔP were set. An optimization algorithm is applied in the program to find the theoretical profile that best matches the drop profile exacted from the image by varying the three initial guess values (for detail, see Ref. 15). For the polynomial fitting method, a percentage of the detected drop profile is used to fit a second order polynomial.^{16,19}

B. Hardware subsystem

To properly conduct the surface contact angle measurement, besides the smartphone, additional associated hardware is needed (note that using the smartphone without hardware can still provide contact angle values, but with less accuracy and is not recommended for scientific work). Figure 4 shows the arrangement of the hardware. The hardware consists of four parts, a base for holding the smartphone, a liquid drop injection system, a stage which can level the solid surface, and a light-emitting diode (LED) defused back light. A 500 μl threaded plunger syringe is used for the drop

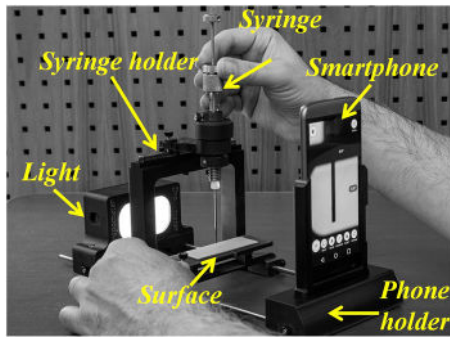


FIG. 4. Arrangement of the smartphone-based contact angle measurement instrument.

generation. As shown in Fig. 4, all five parts are connected with two rods, which allow the user to adjust the position of each of the parts to fulfil different experiment requirements (e.g., change in lighting or to accommodate for optical characteristic of different smartphones, etc.). LG-G5 smartphone [CPU: Snapdragon 820, Screen size: 5.3 in., random access memory (RAM): 4 GB, and Storage: 32 GB] was selected as a test bed for the developed methods. It should be pointed that our methodology is not bounded to LG-G5 smartphone. Any other smartphone available can be used as we have run and tested the software with different smartphones, similar to our earlier work.¹⁸

As can be seen in Fig. 4, the hardware can be dissembled very easily since each of the components can be disconnected from the rod, by loosening a setscrew and sliding the component out of the two rods. This modular design can make the hardware very flexible as to add or remove any component desired to allow for flexible implementation of the system into other apparatus (see, for example, Sec. II C). Such a modular design can also allow changing any of the components without the need for major alterations to the hardware (e.g., in the future, if one wants to add an environmental chamber to conduct contact angle measurement in high temperature environment).

C. Experiments

To test the performance of this instrument, the contact angle between distilled water and five different solid surfaces is measured. The surfaces are glass, poly (methyl methacrylate) (PMMA), polystyrene (PS), Teflon AF, and superhydrophobic (SH). The glass and PMMA surfaces are hydrophilic surface (contact angle with water less than 90°). The PS surface has the contact angle value around 90° . Teflon AF and SH surfaces have contact angles larger than 90° . Therefore, these five surfaces cover the range of the contact angles normally used in various research/development, quality control, and education activities. In this study, plain microscope slides which were cleaned by acetone first and then distilled water were used as the glass surface. The PMMA, PS, and Teflon AF surfaces were fabricated using the spin coating method with a polished aluminum plate as the substrate. The SH surface was prepared by coating Teflon AF on an acid etched aluminum substrate.

The measurement results from the smartphone instrument were compared with the results obtained from a commercial

instrument (Krusz DSA100E), which is considered currently as a high-end measurement instrument. Two different comparisons were performed. First, we used both instruments to measure the contact angle of the same liquid drop on the same surface simultaneously and compared the measurement results. For each of the measurements, a $50 \mu\text{l}$ water drop was generated on the surface using the commercial instrument. Note that due to modular nature of our hardware in these experiments, the drop generation and surface holder components were removed. Drop image (without needle) was taken simultaneously by both the camera of commercial instrument and the smartphone (with a back light) with perpendicular perspectives to each other. For each surface, three measurements were done.

In the second measurement, the advancing and receding contact angles of water on a solid surface was measured separately by using both the commercial and smartphone instruments. The initial liquid drop volume for the both instruments was set to be $50 \mu\text{l}$ with the liquid injection/suction speed of $3 \mu\text{l/s}$. Since the liquid injection system is operated manually, for the smartphone instrument, the liquid volume and liquid injection/suction speed were controlled by counting the number of revolution and twisting speed of the syringe threads, respectively. For each surface, three measurements on different locations of a particular surface were performed.

III. RESULTS AND DISCUSSION

We first tested the software subsystem of the instrument by measuring the contact angle of synthetic drops. Synthetic drops were generated by axisymmetric liquid-fluid interfaces (ALFI) program,¹⁵ which can numerically generate an ideal sessile drop profile based on the Young-Laplace equation. Once the synthetic drop was generated, the drop profile was treated as a detected edge by the software. Both the Young-Laplace and

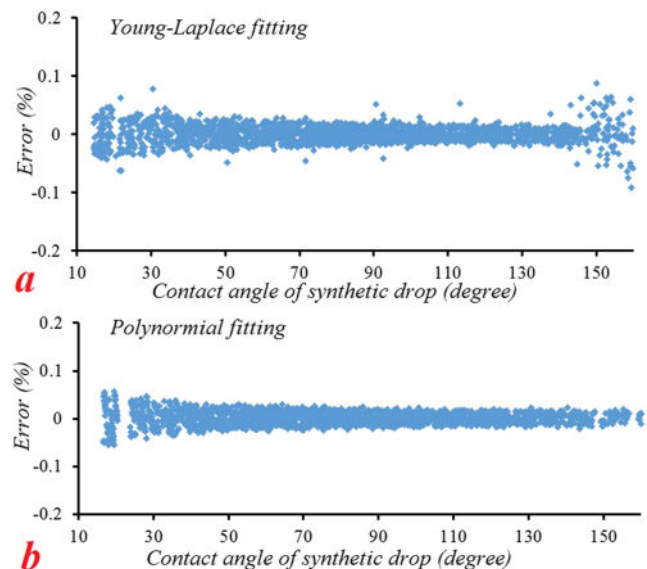


FIG. 5. Error value for (a) the Young-Laplace and (b) the polynomial methods. For each method, 2049 synthetic drops were used. Three measurements for each drop were conducted.

TABLE I. Summary of the error for synthetic contact angle measurements using both the Young-Laplace and Polynomial fitting methods.

Fitting method	Average error (%)	Median error (%)	Maximum error (%)
Young-Laplace	0.01	0.01	0.09
Polynomial	0.01	0.01	0.06

the polynomial fitting methods were used for the measurement analysis. The difference between the measured contact angles and the corresponding synthetic drop contact angle was considered as the error of the measurement. In total, 2049 synthetic drops with contact angles between 10° and 162° were generated. The volume of these drops varied between $0.02 \mu\text{l}$ and $50 \mu\text{l}$. For each drop, three replicate measurements were performed.

We found that the three measurement results for the same drop were identical. So for the synthetic drops, the precision was perfect but accuracy (errors) for the measurements is shown in Fig. 5. Figure 5 shows the percentage error (error divided by the value of the corresponding contact angle for the synthetic drop) for both Young-Laplace and polynomial methods. The errors for the measurements are summarized in Table I. It can be seen that both methods provided good measurement accuracy and precision. The average error of both Young-Laplace and Polynomial fitting methods is 0.01% , suggesting 0.01% accuracy of measurement among these synthetic drops can be achieved. The results shown in Fig. 5 confirm that the smartphone-based instrument can very accurately measure the contact angle with synthetic drops (note the usual accuracy of the contact angle is quotes at 1° , i.e., a minimum accuracy of 0.56% over full range, i.e., 180°).

Further performance tests were conducted by comparing the contact angle measurement results with the ones from a high-end commercial instrument. Table II shows the comparison between the results from the system based on the smartphone and the commercial instrument for the simultaneously measured contact angles by imaging one and the same drop, but from perpendicular optical axes. In general, good agreement between the results from two instruments can be seen. Small deviation of the measurement results was found when the polynomial method was used. The differences of the polynomial method could be caused by the fact that the drop is not perfectly axisymmetric. Although the drop is generated very carefully, it is very typical due to a variety of factors, e.g., minute imperfection of a surface such as inhomogeneity, the drop will not be perfectly axisymmetric. Therefore, the contact angle of the drop along the contact line can be slightly different. From Table II, it is of interest to observe that the measurement results from the Young-Laplace fitting between the two instruments have a better consistency than that of the polynomial fitting method. This is so as different portions of the experimental drop profile are used for the two fitting methods. The Young-Laplace fitting method uses the whole drop profile to calculate the contact angle value, whereas polynomial fitting uses a certain percentage (see Fig. 2) of the drop profile. The Young-Laplace fitting method can underplay the local difference as stated earlier. Therefore, the measurement results from Young-Laplace methods are less affected by the surface imperfection locally. The results shown in Table II confirm that the smartphone-based instrument can work well with the images of a drop without a needle inserted in the drop.

TABLE II. Comparison between measurement results from commercial and smartphone instruments (simultaneous measurements). For each of the surfaces, three different drops were used; note the values shown are for static (or as placed) contact angles.

Surface/drop name	Young-Laplace method		Polynomial method	
	Smartphone results (deg)	Commercial instrument results (deg)	Smartphone results (deg)	Commercial instrument results (deg)
Glass 1 ^a	39.3	39.5	41.7	37.4
Glass 2	37.1	37.8	40.3	36.6
Glass 3	36.9	37.7	37.2	36.8
PMMA 1	74.3	73.8	75.9	73.1
PMMA 2	72.3	73.7	75.1	72.7
PMMA 3	72.7	73.1	73.0	72.3
PS 1	95.5	95.6	92.1	92.5
PS 2	90.3	90.9	89.6	89.7
PS 3	90.0	90.8	88.1	89.7
Teflon AF 1	122.0	123.3	119.5	123.2
Teflon AF 2	119.7	119.9	119.4	118.8
Teflon AF 3	121.8	123.5	119.3	121.7
SHS 1	149.3	152.4	148.2	149.8
SHS 2	156.5	158.8	149.3	154.3
SHS 3	156.4	154.4	145.5	150.5

^aThe contact angle between pure water and smooth glass (ideally) should be close to zero. The relatively large value of the contact angle on glass ($\sim 37^\circ$) can be caused by the imperfection of the glass surface. The variations of the absolute value of the glass contact angle from the ideal situation do not change the fact that the measurement results from the two instruments match with each other.

TABLE III. Comparison between measurement results from commercial and smartphone instruments (advancing and receding contact angle measurement). For each of the surface, three different drops were used. The reported values are the average value of three measurements.

Surface name	Advancing contact angle		Receding contact angle	
	Smartphone results (deg)	Commercial instrument results (deg)	Smartphone results (deg)	Commercial instrument results (deg)
Glass	46.1 ± 1.5	45.1 ± 2.3	19.05 ± 1.4	19.3 ± 3.0
PMMA	76.3 ± 1.5	76.5 ± 0.7	57.6 ± 1.9	55.7 ± 1.4
PS	108.3 ± 1.8	107.6 ± 1.1	69.0 ± 2.8	67.5 ± 1.0
Teflon AF	124.8 ± 1.2	123.1 ± 2.9	110.3 ± 2.8	110.2 ± 1.5
SHS	150.12 ± 2.8	152.92 ± 1.7	148.3 ± 3.1	150.1 ± 2.7

To evaluate the performance of the instrument with a needle inserted into the drop to allow for advancing and receding contact angle measurements, five solid surfaces were used. In these measurements, due to the presence of the needle, the liquid drop is not perfectly axisymmetric; hence, only the polynomial fitting method was used for the measurement and comparison. The measurement results from both smartphone and the commercial instruments are shown in Table III. It can be seen that almost identical results were obtained from the two instruments (considering the error bars). Therefore, we can conclude that the smartphone-based instrument is matching the performance of a top traditional measurement instrument. The successful demonstration of use of a smartphone to conduct contact angle measurement is a significant advancement in the field as it breaks the dominate mold of use of a computer and a bench bound setup for such systems since their appearance in 1980s.²⁰

IV. CONCLUSION

In this study, a smartphone (mobile phone) based contact angle measurement instrument was developed and tested. Compared with the traditional measurement instruments, this instrument has the advantage of small size, portability, and simplicity. The accuracy of the new system with ideal synthetic drop profiles can reach 0.01% with both Young-Laplace fitting and polynomial fitting methods. We compared the measurement results (for both static and dynamic contact angle measurements) between this smartphone-based instrument and traditional commercial instruments and showed good agreement between the results. We conclude that the smartphone-based instrument is matching the performance of a top traditional measurement instrument.

ACKNOWLEDGMENTS

We thank Mr. Glib Sitiugin and Mr. Gurdeep Saini for their help in the instrument development. The assistance of Mr. Saeid Shakeri for preparing some of the images is acknowledged. The financial support of NSERC is also acknowledged by the authors.

¹D. Y. Kwok and A. W. Neumann, "Contact angle measurement and contact angle interpretation," *Adv. Colloid Interface Sci.* **81**, 167–249 (1999).

²O. I. Rio, D. Y. Kwok, R. Wu, J. M. Alvarez, and A. W. Neumann, "Contact angle measurements by axisymmetric drop shape analysis and

an automated polynomial fit program," *Colloids Surf., A* **143**, 197–210 (1998).

³H. Chen, N. Tabatabaei, and A. Amirfazli, "Liquid bridge as a tunable-focus cylindrical liquid lens," *Appl. Phys. Lett.* **110**, 041608 (2017).

⁴G. Liang and I. Mudawar, "Review of drop impact on heated walls," *Int. J. Heat Mass Transfer* **106**, 103–126 (2017).

⁵W. Yao, K. Bae, M. Jung, and Y. Cho, "Transparent, conductive, and superhydrophobic nanocomposite coatings on polymer substrate," *J. Colloid Interface Sci.* **506**, 429–436 (2017).

⁶S. Moradi, P. Englezos, and S. G. Hatzikiriakos, "Contact angle hysteresis of non-flattened-top micro/nanostructures," *Langmuir* **30**, 3274–3284 (2014).

⁷C. N. C. Lam, R. Wu, D. Li, M. L. Hair, and A. W. Neumann, "Study of the advancing and receding contact angles: Liquid sorption as a cause of contact angle hysteresis," *Adv. Colloid Interface Sci.* **96**, 169–191 (2002).

⁸J. Drelich, J. D. Miller, and R. J. Good, "The effect of drop (bubble) size on advancing and receding contact angles for heterogeneous and rough solid surfaces as observed with sessile-drop and captive-bubble techniques," *J. Colloid Interface Sci.* **179**, 37–50 (1996).

⁹D. K. Mandal, A. Criscione, C. Tropea, and A. Amirfazli, "Shedding of water drops from a surface under icing conditions," *Langmuir* **31**, 9340–9347 (2015).

¹⁰A. Marmur, C. D. Volpe, S. Siboni, A. Amirfazli, and J. W. Drelich, "Contact angles and wettability: Towards common and accurate terminology," *Surf. Innovations* **5**(1), 3–8 (2017).

¹¹L. M. Lander, L. M. Siewierski, W. J. Brittain, and E. A. Voglert, "A systematic comparison of contact angle methods," *Langmuir* **9**, 2237–2239 (1993).

¹²O. N. Tretinnikovt and Y. Ikada, "Dynamic wetting and contact angle hysteresis of polymer surfaces studied with the modified Wilhelmy balance method," *Langmuir* **10**, 1606–1614 (1994).

¹³J. Drelich, "Guidelines to measurements of reproducible contact angles using a sessile-drop technique," *Surf. Innovations* **1**(4), 248–254 (2013).

¹⁴A. F. Stalder, G. Kulik, D. Sage, L. Barbieri, and P. Hoffmann, "A snake-based approach to accurate determination of both contact points and contact angles," *Colloids Surf., A* **286**, 92–103 (2006).

¹⁵O. I. Rio and A. W. Neumann, "Axisymmetric drop shape analysis: Computational methods for the measurement of interfacial properties from the shape and dimensions of pendant and sessile drops," *J. Colloid Interface Sci.* **196**, 136–147 (1997).

¹⁶A. Bateni, S. S. Susnar, A. Amirfazli, and A. W. Neumann, "A high-accuracy polynomial fitting approach to determine contact angles," *Colloids Surf., A* **219**, 215–231 (2003).

¹⁷D. Williams, A. Kuhn, T. O. Bryon, M. Konarik, and J. Huskey, "Contact angle measurements using cellphone cameras to implement the Bikerman method," *Galvanotechnik* **8**, 1718–1725 (2011).

¹⁸H. Chen, J. L. Muros-Cobos, J. A. Holgado-Terriza, and A. Amirfazli, "Surface tension measurement with a smartphone using a pendant drop," *Colloids Surf., A* **533**, 213–217 (2017).

¹⁹S. F. Chini and A. Amirfazli, "A method for measuring contact angle of asymmetric and symmetric drops," *Colloids Surf., A* **388**, 29–37 (2011).

²⁰Y. Rotenberg, L. Boruvka, and A. W. Neumann, *J. Colloid Interface Sci.* **93**(1), 169–183 (1983).